Design of a Coriolis Acceleration Experimental Device

Hafizan Hashim, Hanita Hashim

Abstract*: Important drawbacks of Coriolis experimental setup and devices are their multiple parts and cost to own. Simplicity, traceability, and measurability are the major concern. This paper presents a preliminary design process of Coriolis acceleration experimental device to visualize the effect of Coriolis and enable the calculation of acceleration components to facilitate students for a better understanding of this phenomenon. This is realized through a slidable collar with a marker and accelerometer attached on it and a rotating rod that shows a visible yet erasable mark from the marker's path. The design process went through typical engineering design processes such as morphological study, functional decomposition, and Pugh chart. Next, Finite Element Analyses (FEA) were performed to determine the mode shapes, followed by analytical calculation of the dynamic reaction experienced by motor. In addition, this kit provides opportunity for students to manually calculate the actual acceleration component based on theory learnt which is considered innovative. The use of controllable motor for rotating the rod could vary the travelling path of the marker, subsequently diversify the problems for student to solve.

Keywords* : Coriolis acceleration, inertia frame, rotating rod, travelling path

I. INTRODUCTION

The Coriolis effect is the deflection of moving objects in a confusing way when they are viewed in a rotating reference frame. In physics, the Coriolis force is an inertial force that acts on objects that are in motion relative to a rotating reference frame. In a reference frame with clockwise rotation, the force acts to the left of the motion of the object. In one with anticlockwise (or counterclockwise) rotation, the force acts to the right. Deflection of an object due to the Coriolis force is called the Coriolis effect. Machines and mechanisms running at a high speed are considered by a kinematic analysis of their velocities and accelerations, and subsequently analyzed as dynamic systems in which forces due to accelerations are analyzed using the principles of kinetics. Force and stress analysis is based on the acceleration analysis of links and points of interest in the mechanism or machine. In classical mechanics there are many ways to derive equations of accelerations. The Coriolis acceleration is an acceleration which, when added to the acceleration of an object relative to a rotating coordinate system to its centripetal acceleration, gives the acceleration of the object relative to a fixed coordinate system.

The Coriolis effect has always been subject to confusion. Misunderstandings and misleading explanations on this phenomenon have been common. Even today, with all our knowledge in physics, these errors seem to occur everywhere - in lecture halls, throughout textbooks and in academic journals. However, the Coriolis effect is somewhat difficult to explain and understand. It is not the mathematics that causes confusion; the algebraic derivations of the phenomenon are quite straightforward, it is the conceptual explanation of what actually happens that is hard to understand. Most systems that exist today are developed only for visualizing the Coriolis effect without considering that it may be desirable to capture or record the phenomenon for later analysis or use. This could possibly be the cause for lack of understanding regarding the phenomenon among students. This section reviews some of the patented devices for demonstrating the action of Coriolis force. There is abundance of information available pertinent to the Coriolis devices, however, mostly are regarded to fluid measuring instruments. Table I shows summary of some patented devices including the recent ones.

In general, all these innovations may have a direct impact on the learning outcomes of the students. However, there is room for improvement in some of the innovations described earlier. Detail comparison in terms of safety, cost, and maintainability could not be done due to lack of information on those devices. Authors believe that present preliminary design has some advantages in terms of cost, safety, complexity, and maintainability which current designs do not have. The objective of this work is to generate preliminary design of the Coriolis device, perform computer simulation, and determine some of the dynamic properties for part selection. Using typical engineering process design, it starts with morphological, functional decomposition, and Pugh chart. Rotor type design with slider is preferred over others after some considerations on safety, cost, and technical feasibility were imposed. Next, simulations of mode shapes were conducted using finite element software followed by calculation of equation of motion to determine the minimum requirement of the motor.

Revised Manuscript Received on 10 October, 2019.
***** Correspondence Author
Hafizan Hashim*, Faculty of Mechanical Engineering, Universiti Teknologi MARA, 40450 Shah Alam, Selangor, Malaysia. Email: hafizandes@gmail.com
Hanita Hashim, Faculty of Engineering and Life Siences, Universiti Selangor, Berjuntai Bestari, Malaysia. Email: hanita@unisel.edu.my

Table I. Summary of some patented device

No	Doc. ID No. / Inventor (s)	Status	Title	Mechanism and drawing (s)	Ref.
1	RU2078378C1 N.V. Butenin, L.D. Ivanov, A.V. Chizhov, R.V.Sokhabeyev	Patent grant	Device for demonstration of action of Coriolis inertia force.	This device consists of a base, stand, guided stopper, and a fixed mass. The wheel type mass rotates on spherical bearings and the axle is kinematically coupled with the slide. The wheel will start moving when the guides rotate, causing the wheel to accelerate at certain value and direction. A lever mounted on the drive shaft is used to visualize the action of the Coriolis force. It consists of two (2) parts, cylindrical and frusto-conical tubes, and ball bearings are placed in the tubes as the moving objects.	Year: 1997 [1]
2	CN2672784Y Lu Junling, Wang Rongbao	Patent grant	Concave surface Coriolis force rotary disc demonstration test instrument 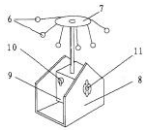 Fig. 1: Overall view	This device consists of a rotating disc with some ball bearings hanging around (pendulum-liked) as shown in Fig. 1. As the disc rotates, pendulums will form a concave surface from side view. The concave angle that indicates different acceleration components acting on ball bearings changes with angular velocity of the disc. Effect of varying the angular velocity of the disc on the Coriolis force could be seen throughout the experiment. This device can be operated manually by turning the dial instead of using motor.	Year: 2005 [2]
3	CN100487752C We Wenlong, Y. Z. Ming Z. Niwang Y. Weijian, C. Jianping	Patent grant	Coriolis force experimental equipment	This device consists of a sliding mass in a guide rail mounted on a rotating disc. As the disc rotates, position of the mass in the guide rail will be controlled to visualize the Coriolis effect. The disc is equipped with angle sensor and limit switch for safety purpose. The guide rail is equipped with load cell to measure the force components acting during rotation. The guide rail does not experience force on *x*-axis but *y* and *z* direction.	Year: 2009 [3]
4	CN101625805B Zhu Chengjiu, Zhu Aihua	Patent grant	Coriolis acceleration test device 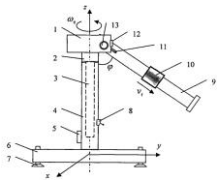 Fig. 2: Front view	This device consists of a main frame with a fixed support column that carries a motor on its top to produce a rotation. A rod with a slidable mass is attached to the rotary node using hinge mechanism to allow the rod to elevate vertically. The motor is controllable and rotates around the *z*-axis as shown in Fig. 2. It is equipped with angle and linear dispalcement sensor. A two-sided strain gauge is attached to the one end of the rod and all sensors are connected to a signal processing unit for analysis.	Year: 2011 [4]

5	CN201927245U Yan Yongwei, Wang Hao	Patent grant	Stereoscopic mechanical belt type Coriolis acceleration test instrument	This stereoscopic mechanical belt type Coriolis acceleration test device has two (2) simultaneous rotational motion. The plane motion which rotates vertically produces relative motion and at the same time the horizontal rotation rotates the vertical plane motion and both are mutually perpendicular and independent. The vertical belt wheel can transversely move on the cylindrical belt wheel to visualize the Coriolis effect. Both angular velocities, vertical and horizontal rotations, are controllable.	Year: 2011 [5]
6	CN203931271U Wang Jie, Zhao Ya Zhou, Hao Long, Yang Yang, Waang Wei	Patent grant	Coriolis acceleration experimental device	This device consists of rotary and linear motion mechanisms and both are placed on a rigid base. A motor producing the rotational motion is connected to a vertical shaft using a belting system and a guide rail equipped with mass-pulley system is attached to the rotating shaft. The Coriolis effect can be observed and analyzed quantitatively through sensors installed in the system.	Year: 2014 [6]
7	CN204257073U Wang Xiao Tong, Zhang Mian Hao	Patent grant	Coriolis acceleration demonstration apparatus 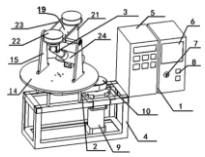 Fig..3: Overall view	This device consists of rotational motion and relative motion assemblies. A motor is connected to a rotating table that carries the relative motion assembly using drive belt. The assembly consists of a support frames and shafts, bearings, motor, wheels, and belt. All sensors are connected to the computer as shown in Fig. 3 for further analyze the Coriolis acceleration.	Year: 2015 [7]
8	CN204720047U Liu et al.	Patent grant	Coriolis acceleration demonstration appearance	This device is a combination of rotational and linear motions. A disc with linear motion track is attached on a vertical rotating shaft which is belt-connected to a motor. The effect of Coriolis on the slidable mass could be observed when the disc rotates. This device provides visualization of Coriolis effect for a better understanding of the concept.	Year: 2015 [8]
9	CN103943004B Z. S. Song, L. Peng, W. W. Hua, Y. D. Ping, Jin Jian, Xia Hang	Patent grant	Coriolis acceleration test device	This device consists of a rotating circular bench and a screw type linear actuator. The linear actuator carries position sensor with a mass which can be reposition linearly. As the bench rotates, the Coriolis force will take effect and produces some measurement. This device can also be used for position control of the slidable mass for balancing the rotating circular bench.	Year: 2016 [9]

10	CN104021708B Pi Wei, S.C. Ming, Liu Yue, Liu Jie, X. Xinyu, Z. Jianmin, Q.Wei, W.X.Hua	Patent grant	Demonstrator Coriolis acceleration and Coriolis inertia force measurement method	This device consists of a rotating circular bench with controlled slidable collars. The two (2) collars which are positioned on one side each are controlled using a motor and a wheel-belts system which is mounted perpendicular and centered to the linear rail. Load cells and displacement sensors are attached on both collars.	Year: 2016 [10]
11	CN104361791B Duan Jie Li, X. P. Hui, L. R. Fu, Z. Z. Ho, W. Shuo, T. J. Xin, W. Y. Yu	Patent grant	One kind of Coriolis acceleration demonstrator	This device consists of a rotating test platform made of a disc plate. A motor is connected to the vertical rotating shaft using belted-wheel to rotate the round platform. On the platform, mounted two (2) more motors with ball screw linear drivers which are used to control the position of sliders. Those motors are controlled wirelessly. The sliders are equipped with load cells and displacement sensors. All sensors are connected to a computer for further analyze the Coriolis phenomena.	Year: 2016 [11]
12	CN104751707B Liu Ming, Liu Yi Ming, Wu Yong Chao, Luo Wei, Ma Hong Jian, Wei Hao Xiang, Teng Wei	Patent grant	Coriolis acceleration demonstrator 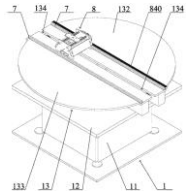 Fig. 4: Overall view	This device is a combination of rotational and linear motions. A disc with linear motion track is attached on a vertical rotating shaft which is belt-connected to a motor as shown in Fig. 4. The effect of Coriolis on the slidable mass could be observed when the disc rotates. Under the action of first motor (rotation) and second motor (translation), the position and forces acting on the slider could be detected simultaneously. This device provides visualization of Coriolis effect for a better understanding of the concept.	Year: 2017 [12]
13	CN1048353888 B W. P. Kai, L. R. Jiang, Z. Chao, Z. Y.Chao, Z. Bin, J.Wen, Lu Xu, Z. Peng, Y. X. Feng, G. X.Liang, Bai Jun Feng, Li Hua, Xu Bing	Patent grant	Based presentation and calculation method and apparatus of the Coriolis acceleration physics simulation form 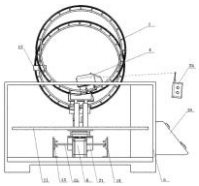 Fig. 5: The front view	The present invention consists of a rotating circular bench plate with two (2) vertical circular rails as shown in Fig. 5. A rotary slider or rail car is attached to the rail and can freely slide in rotational motion on the rail track. A motor is connected to the circular bench using belted-wheel system and a vertical shaft. Accelerometers were attached on two (2) different places, 1) fixedly mounted on the round track and wired to microcontroller with control panel, 2) on the slider or rail car. The speed of the slider would be measured using electromagnetic induction.	Year: 2017 [13]
14	CN206400899U Zhang	Patent grant	Coriolis acceleration demonstrator 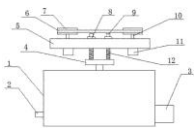 Fig. 6: The side view.	This device consists of a base, supporting bench, rotating disc, wheels, belts, and motors as shown in Fig. 6. Motor in the base is connected to to the vertical rotating shaft using worm gear to rotate the disc. Relative motion occurs when one of the motor mounted on the rotating disc rotates simultaneously with the disc. Due to Coriolis effect, the belt system connecting the two (2) motors will be streched or vice versa depending on the direction of rotation of the disc.	Year: 2017 [14]

15	G.U.N.T. Gerätebau GmbH	N/A	TM 605 Coriolis force	This device consists of a rotating water tank which is driven from a geared-belting motor with submersible pump. The pump is attached on a rotatable arm to produce a water jet in radial direction during rotation. The deflection of the water jet due to the Coriolis effect depends on the flow rate, speed and direction of the rotation. It can be determined by means of a scale on the water tank. This device capable to clearly demonstrate the Coriolis phenomena in a rotating reference frame.	Yearr: 2018 [15]

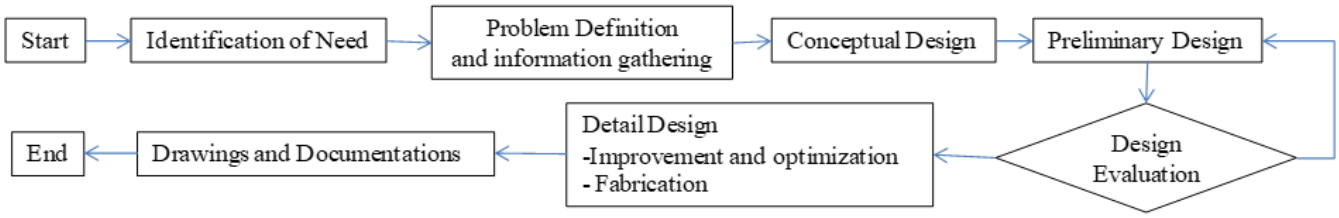

Fig. 7: Design flowchart.

II. METHOD

Fig. 7 shows the overall design flowchart that contains relation between major parts of the system. The engineering design process is an iterative process which is open ended in nature. There is no single solution for the problem and it always evolve over time. Some basic evaluation tools such as Morphological and Pugh Chart are implemented in the design process. Frequency analyses were conducted using ABAQUS and the details are discussed in the later section.

III. RESULTS

Based on the WIPO patent search, some of the similar keywords pertaining to the design were managed to be extracted. All related information has been gathered and analyzed in order to identify the advantages and disadvantages of each patent. This analysis has brought us to the following conclusion on the important criteria for the selection of the preliminary design: 1) Simplicity, 2) Stability, 3) Cost, 4) Controllability, and 5) Traceability. Fig. 2 below shows the morphological chart of the design selection. It links all the available options for the best design combination systematically. All the four options share the basic concept which is a relative motion in a rotating frame.

Fig. 8 and Table III show functional decomposition and Pugh chart respectively. The functional decomposition chart is used to gain insight into the identity of the constituent parts or components that represents their specific function. It helps designer to identify the simplest components to work with for the application and helps identify the complex and/or risk areas of the project. The Pugh matrix is a qualitative selection to make fast qualitative comparisons by comparing an option against a datum or reference option. It is a comparison between current options with respect to datums or particular criteria. The option could be the same as the datum condition or possibly better than the dead-end condition or worse than the datum condition. Next, general evaluations are performed and summarized then the preference approach is determined.

As shown in Table II, according to net score, design 4 is preferable over others.

Table II. Summary of some patented device

	Option 1	Option 2	Option 3	Option 4
Mechanism		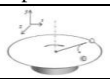	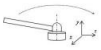	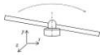
Tracker / Traceability	N/A	YES	YES	YES
Object in motion	Slider	Ball bearing	Slider	Slider
Encoder	YES	YES	YES	YES
Accelerometer	YES	N/A	YES	YES

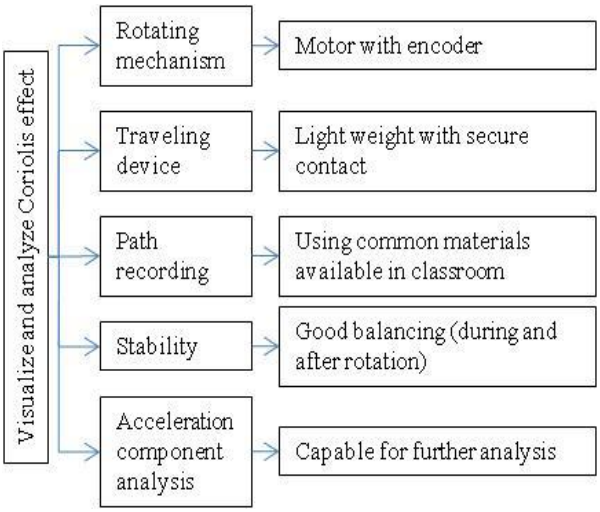

Fig. 8: Functional decomposition chart.

Table III. Pugh Chart

Description			Design 1	Design 2	Design 3	Design 4
Criteria	Weight	Datum				
Size	1	0	+	+	+	-
Weight	2	0	+	+	+	+
Stability	5	0	+	+	-	+
Traceability	5	0	0	+	+	+
Measurability	5	0	0	-	+	+
Cost	1	0	0	+	0	0
Maintainability	2	0	-	+	-	0
Simple design	2	0	-	+	0	0
+			3	7	5	5
0			3	0	1	2
-			2	1	2	1
Net score			4	13	6	16

Fig. 9 shows the isometric view of the preliminary design of the Coriolis kit. It consists of a double rod with a stopper at each end, a slider mounted with marker and accelerometer, a vertical driving shaft connected to the rotor, and a servo motor. The slider and marker are used to visualize and sketch the traveling path of the slider respectively.

The accelerometer measures proper acceleration of the slider in its own instantaneous rest frame. In one embodiment, the two (2) cylindrical rods are secured at center and both ends and they act like a helicopter rotor blade. Compared to cantilevered type as shown in Option 3 of Table II, this type of rotor is more stable and manageable. Proper lubrication is crucial importance for a smooth translation of the slider. Regardless of the particular embodiment, it will be understood by those knowledgeable and skilled in the art that the device advantageously employs controllable motor and traceable travelling path of slider to enable manipulation of angular speed and effectively utilize analytical technique for solving the problem in acceleration analysis. Other features, objects, and advantages of the present invention will be apparent to those of ordinary skill in the relevant arts.

A. Mode shapes

The device consists of a double rotating rods that may shake during the motion. In this work, finite element method is used to perform the natural mode shapes and frequencies analysis. The mode shapes are the fixed properties possessed by an object and the most desired modes are mostly the lowest frequencies which dominate all the higher frequency modes. The lowest frequencies can be the most prominent modes at which the object will vibrate. This device is not intended to be used for a long period of rotation, however identifying the resonance mode shapes could be the early stage of structural fault identification. Fig. 10 shows the lower frequencies mode shape of the device.

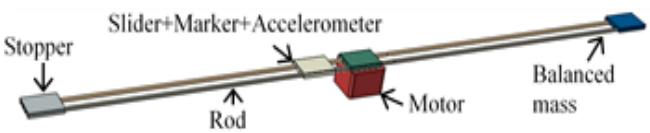

Fig. 9: Isometric view of the preliminary design.

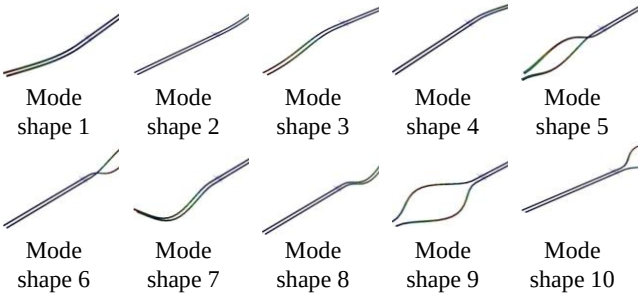

Fig. 10: Mode shapes.

B. Dynamic reaction

The forces and moments of forces acting on a rigid body may cause complex three-dimensional motion of that body. When an external force is applied to a rotating body, the resulting displacement may be in a different direction from that of the force. The reason for this phenomenon is that the change in direction of the angular velocity vector involves an angular acceleration. This concept deals with the kinematics of rigid bodies, and is used here for analyzing the motion of bodies when the instantaneous axes of rotation change. The fundamental equations of motion for any rigid body are given by (1) and (2).

$$\sum \vec{F} = m\vec{a}_c \tag{1}$$

$$\sum \vec{M}_c = \dot{\vec{H}}_c \tag{2}$$

where $\vec{a}_c$ is the acceleration of the center of mass and $\dot{\vec{H}}_c$ is the angular momentum of the body about its center of mass. (2) may also be used with any fixed point *O* for a reference if both $\sum \vec{M}$ and $\vec{H}$ are evaluated about that point. The greatest difficulty in using these apparently simple equations is in obtaining derivatives of the angular momentum $\vec{H}$. $\vec{H}$ is defined for a particular position of the body with respect to axes of fixed orientation. At a different time and position, the body's mass moments and products of inertia may be different with respect to the same fixed frame. Thus, differentiation of angular momentum is possible only if it is given as a function of time. However, this problem can be solved using fixed reference axes attached at the mass center of the body. The maximum number of independent scalar equations of motion of a rigid body is six. They are presented here as a group of governing equations for convenience.

$$\sum F_x = ma_{c_x} \quad \sum F_y = ma_{c_y} \quad \sum F_z = ma_{c_z} \tag{3}$$

$$\sum M_x = \dot{H}_x + \omega_y H_z - \omega_z H_y, \sum M_y = \dot{H}_y + \omega_z H_x - \omega_x H_z \quad \sum M_z = \dot{H}_z + \omega_x H_y - \omega_y H_x \tag{4}$$

The xyz axes fixed in the body and rotating with it may be chosen to coincide with the principle axes of inertia of the body with respect to the mass center *C* or a fixed point *O*. In this way, all the products of

inertia will be zero, thus $\bar{I}_{xy} = \bar{I}_{yz} = \bar{I}_{zx} = 0$. $\dot{\vec{H}}_c$ is now become:

$$\dot{\vec{H}}_c = \left(\bar{I}_x\dot{\omega}_x\vec{\imath} + \bar{I}_y\dot{\omega}_y\vec{\jmath} + \bar{I}_z\dot{\omega}_z\vec{k}\right) + \vec{\omega}\times\vec{H}_c \quad (5)$$

Simplifying (5) to obtain:

$$\begin{aligned}\dot{\vec{H}}_c = {} & \left[\bar{I}_x\dot{\omega}_x - (\bar{I}_y - \bar{I}_z)\omega_y\omega_z\right]\vec{\imath} + \\ & \left[\bar{I}_y\dot{\omega}_y - (\bar{I}_z - \bar{I}_x)\omega_z\omega_x\right]\vec{\jmath} + \\ & \left[\bar{I}_z\dot{\omega}_z - (\bar{I}_x - \bar{I}_y)\omega_x\omega_y\right]\vec{k} = M_x\vec{\imath} + M_y\vec{\jmath} + M_z\vec{k}\end{aligned} \quad (6)$$

where:

$$\begin{aligned}M_x &= \bar{I}_x\dot{\omega}_x - (\bar{I}_y - \bar{I}_z)\omega_y\omega_z \\ M_y &= \bar{I}_y\dot{\omega}_y - (\bar{I}_z - \bar{I}_x)\omega_z\omega_x \\ M_z &= \bar{I}_z\dot{\omega}_z - (\bar{I}_x - \bar{I}_y)\omega_x\omega_y\end{aligned} \quad (7)$$

These equations are known as *Euler's equation of motion* and can be used to analyze the motion of a rigid body about its mass center *C*. Using principle axes *x*, *y*, *z* as shown in Fig. 11, moments of inertia:

For C1: $\bar{I}_{x(C1)} = \frac{1}{12}m(b^2 + c^2)$, $\bar{I}_{y(C1)} = \frac{1}{12}m(a^2 + c^2)$, $\bar{I}_{z(C1)} = \frac{1}{12}m(a^2 + b^2)$

For C2: $\bar{I}_{x(C2)} = \frac{1}{12}m(b^2 + c^2)$, $\bar{I}_{y(C2)} = \frac{1}{12}m(a^2 + c^2) + m(0.48)^2$, $\bar{I}_{z(C2)} = \frac{1}{12}m(a^2 + b^2) + m(0.48)^2$

For C3: $\bar{I}_{x(C1)} = \frac{1}{12}m(b^2 + c^2)$, $\bar{I}_{y(C1)} = \frac{1}{12}m(a^2 + c^2)$, $\bar{I}_{z(C1)} = \frac{1}{12}m(a^2 + b^2)$

For R1: $\bar{I}_{x(R1)} = m(9)^2$, $\bar{I}_{y(R1)} = \frac{1}{12}m_{(R1)}l^2 + m_{(R1)}(9)^2$, $\bar{I}_{z(R1)} = \frac{1}{12}m_{(R1)}l^2 + m_{(R1)}(9)^2$

For R2: $\bar{I}_{x(R2)} = m(9)^2$, $\bar{I}_{y(R2)} = \frac{1}{12}m_{(R2)}l^2 + m_{(R2)}(9)^2$, $\bar{I}_{z(R2)} = \frac{1}{12}m_{(R2)}l^2 + m_{(R2)}(9)^2$

Entire machine part:

$$\bar{I}_x = \frac{1}{12}m(b^2 + c^2) + \frac{1}{12}m(b^2 + c^2) + \frac{1}{12}m(b^2 + c^2) + m(9)^2 + m(9)^2$$

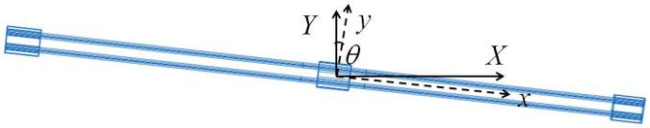

Fig. 11: Body under rotation about principle axes *x*, *y*, *z*.

$$= \frac{1}{4}m(b^2 + c^2) + 2m(9)^2$$

$$\bar{I}_y = \frac{1}{12}m(a^2 + c^2) + \frac{1}{12}m(a^2 + c^2) + m(0.48)^2$$

$$+\frac{1}{12}m(a^2 + c^2) + \frac{1}{12}m_{(R1)}l^2 + m_{(R1)}(9)^2 + \frac{1}{12}m_{(R2)}l^2 + m_{(R2)}(9)^2$$

$$= \frac{1}{4}m(a^2 + c^2) + m(0.48)^2 + \frac{1}{12}m_{(R1)}l^2 + m_{(R1)}(9)^2 + \frac{1}{12}m_{(R2)}l^2 + m_{(R2)}(9)^2$$

$$= \frac{1}{4}m(a^2 + c^2) + m(0.48)^2 + \frac{1}{6}m_{(R)}l^2 + 2m_{(R)}(9)^2,$$

for $m_{(R1)} = m_{(R2)} = m_{(R)}$

$$\bar{I}_z = \frac{1}{12}m(a^2 + b^2) + \frac{1}{12}m(a^2 + b^2) + m(0.48)^2 + \frac{1}{12}m(a^2 + b^2) + \frac{1}{12}m_{(R1)}l^2 + m_{(R1)}(9)^2 + \frac{1}{12}m_{(R2)}l^2 + m_{(R2)}(9)^2$$

$$= \frac{1}{4}m(a^2 + b^2) + m(0.48)^2 + \frac{1}{6}m_{(R)}l^2 + 2m_{(R)}(9)^2$$

Kinematics: $\vec{\imath} = \cos\theta\,\vec{I} - \sin\theta\,\vec{J}$. Since the acceleration of the mass center is zero, the resultant force acting on the vertical rotating shaft which is connected to the motor, is zero. Euler's equation of motion for the assembly:

$$\begin{aligned}M_x &= \bar{I}_x\dot{\omega}_x - (\bar{I}_y - \bar{I}_z)\omega_y\omega_z = 0\ , \\ M_y &= \bar{I}_y\dot{\omega}_y - (\bar{I}_z - \bar{I}_x)\omega_z\omega_x = 0 \\ M_z &= \bar{I}_z\dot{\omega}_z - (\bar{I}_x - \bar{I}_y)\omega_x\omega_y \\ &= \left[\frac{1}{4}m(a^2 + b^2) + m(0.48)^2 + \frac{1}{6}m_{(R)}l^2 + 2m_{(R)}(9)^2\right]\dot{\omega}_z\end{aligned}$$

Therefore, the suitable motor for the system must be able to produce such moment for such angular acceleration.

IV. CONCLUSION

The paper presents the preliminary design and evaluation of the Coriolis kit, a simplified version for educational purposes. Comprehensive patent review has been conducted and the design process went through typical engineering design process. Based on studies and evaluations, design 4 was selected for preliminary simulation and calculation of dynamic reaction. Simulation using finite element software was successfully performed to investigate the mode shapes.

We managed to calculate the minimum moment required for motor selection and dynamic reactions experienced by the rotating shaft which is connected to the motor. This model is practical and useful in providing hands-on experience to student for investigating how the collar moves on the rotating frame due to the Coriolis effect. Compared to existing kit, this model kit not only visualizes the effect but shall also enables manual calculation of acceleration components. Once developed and evaluated for its effects on students' knowledge and self-efficacy, this model kit has the potential to be used not only in classes, but also in laboratories not limited to engineering dynamics.

ACKNOWLEDGEMENT

Authors wishing to acknowledge the Universiti Teknologi MARA (UiTM), IRMI, and FKM of UiTM for providing the Lestari Fund research grant scheme (600-IRMI/MyRA 5/3/LESTARI (023/2017)).

REFERENCES

1. Device for demonstration of action of coriolis inertia force, by L. D. y. I. Nikolay Vasil'yevich Butenin, Aleksey Viktorovich Chizhov, Roman Valer'yevich Sokhabeyev. (1997, April 27). *RU2078378C1.* Accessed on: Feb. 22, 19. [Online]. Available: https://patentscope.wipo.int/search/en/detail.jsf?docId=RU29286986&tab=NATIONALBIBLIO&_cid=P12-JYSB18-62019-1
2. Concave surface conolis force rotary disc demonstration test instrument, by J. L. Lu and R. B. Wang. (2005, Jan 19). *CN2672784Y.* Accessed on: Feb. 20, 2019. [Online]. Available: https://patentscope.wipo.int/search/en/detail.jsf?docId=CN155336507&tab=NATIONALBIBLIO&_cid=P12-JYSDM7-96490-1
3. Coriolis force experimental equipment, by Z. Yan, W. Ni, C. Jianping, Z. Ming, Y. Weijian, and W. Wenlong. (2009, May 13). *CN100487752C.* Accessed on: Feb. 20, 2019. [Online]. Available: https://patentscope.wipo.int/search/en/detail.jsf?docId=CN83117874&_cid=P12-JYSBYN-81714-1
4. Coriolis acceleration test device, by Z. Aihua and Z. Chengjiu. (2011, Nov 16). *CN101625805B.* Accessed on: Feb. 19, 2019. [Online]. Available: https://patentscope.wipo.int/search/en/detail.jsf?docId=CN83819799&_cid=P12-JYSCAN-85289-1
5. Stereoscopic mechanical belt type Coriolis acceleration test instrument, by Y. W. Yan and H. Wang. (2011, Aug 10). *CN201927245U.* Accessed on: Feb. 19, 2019. [Online]. Available: https://patentscope.wipo.int/search/en/detail.jsf?docId=CN156591412&tab=NATIONALBIBLIO&_cid=P12-JYSCS0-89612-1
6. Coriolis acceleration experimental device, by J. Wang, Y. Z. Zhao, L. Hao, Y. Yang, and W. Wang. (2014, Nov 5). *CN203931271U.* Accessed on: Feb. 21, 2019. [Online]. Available: https://patentscope.wipo.int/search/en/detail.jsf?docId=CN158591132&_cid=P12-JYSCZN-91339-1
7. Coriolis acceleration demonstration apparatus, by X. T. Wang and M. H. Zhang. (2015, Apr 8). *CN204257073U.* Accessed on: FEb. 21, 2019. [Online]. Available: https://patentscope.wipo.int/search/en/detail.jsf?docId=CN158920733&_cid=P12-JYSD55-92594-1
8. Coriolis acceleration demonstration appearance, by Y. M. Liu, M. C. Wu, S. L. Luo, H. J. Ma, H. X. Wei, and W. Teng. (2015, Oct 21). *CN204720047U.* Accessed on: Feb. 20, 2019. [Online]. Available: https://patentscope.wipo.int/search/en/detail.jsf?docId=CN159378571&_cid=P12-JYSDAY-93896-1
9. Coriolis acceleration test device, by S. S. Zhang, P. Luo, W. H. Wang, D. P. Yan, J. Jin, and H. Xia. (2016, Apr 13). *CN103943004B.* Accessed on: Feb. 22, 2019. [Online]. Available: https://patentscope.wipo.int/search/en/detail.jsf?docId=CN106894104&_cid=P12-JYSDDG-94504-1
10. Demonstrator Coriolis acceleration and Coriolis inertia force measurement method, by W. Pi, C. M. Su, Y. Liu, J. Liu, X. Xu, J. M. Zhu, *et al.* (2016, June 8). *CN104021708B.* Accessed on: Feb. 22, 2019. [Online]. Available: https://patentscope.wipo.int/search/en/detail.jsf?docId=CN107373534&_cid=P12-JYSDEY-94801-1
11. One kind of Coriolis acceleration Demonstrator, by J. Duan, P. H. Xu, R. F. Li, Z. H. Zhu, S. Weng, J. X. Tan, *et al.* (2016, *CN104361791B.* Accessed on: Feb. 22, 2019. [Online]. Available: https://patentscope.wipo.int/search/en/detail.jsf?docId=CN131125559&_cid=P12-JYSDGS-95237-1
12. Coriolis acceleration Demonstrator, by M. Liu, Y. M. Liu, Y. C. Wu, W. Luo, H. J. Ma, H. X. Wei, *et al.* (2017, *CN104751707B.* Accessed on: Feb. 18, 2019. [Online]. Available: https://patentscope.wipo.int/search/en/detail.jsf?docId=CN145100760&_cid=P12-JYSDIQ-95670-1
13. Based presentation and calculation method and apparatus of the Coriolis acceleration physics simulation form, by P. K. Wang, R. J. Li, C. Zhang, Y. C. Zhang, Z. B. Zhang, B. W. Jiang, *et al.* (2017, Apr 19). *CN104835388B.* Accessed on: Feb. 19, 2019. [Online]. Available: https://patentscope.wipo.int/search/en/detail.jsf?docId=CN196123327&_cid=P12-JYSDK8-96017-1
14. Coriolis Acceleration Demonstrator, by S. Z. Zhang. (2017, Aug. 11). *CN206400899U.* Accessed on: Feb. 22, 2019. [Online]. Available: https://patentscope.wipo.int/search/en/detail.jsf?docId=CN203431021&tab=NATIONALBIBLIO&_cid=P12-JYS8QV-33670-1
15. G. Hamburg. (2019). TM 605 Coriolis force. Available: https://www.gunt.de/en/products/engineering-mechanics-and-engineering-design/dynamics/kinetics-dynamics-of-rotation/coriolis-force/040.60500/tm605/glct-1:pa-148:ca-18:pr-1409

AUTHORS PROFILE

Hafizan Hashim, PhD, is a Senior Lecturer at the Faculty of Mchanical Engineering, Universiti Teknologi MARA (UiTM), Malaysia. He has nearly five years' of working experience in the automotive industries. He is a member of Board of Engineers Malaysia (BEM). His research interests include lightweight structures, structural crashworthiness, optimzation, and vibration control of flexible structures.

Hanita Hashim received a Bachelor of Science (Actuarial Science) (Hons.) from Universiti Kebangsaan Malaysia (UKM), in 2004 and Master of Science (Statistics) from the same university in 2006. Currently she is a lecturer in the Faculty of Engineering and Life Sciences, Universiti Selangor (Unisel) and has more than ten years working experience in teaching and two years as a Program Coordinator. She is a registered member of Malaysia Institute of Statistics. Her research interests include conducting research in social sciences, statistical theory, and optimization. She is currently completing a study entitled *Satisfaction of bus SMART Selangor users* under 'Bestari Grant' funded by State Government of Selangor.